Multimodal radiation impedance of a waveguide with arbitrary cross-sectional shape terminated in an infinite baffle (L)

Rémi Blandin,[1,a)] Annemie Van Hirtum,[2] Xavier Pelorson,[2] and Rafael Laboissière[3]
[1]*GIPSA-Lab, UMR CNRS 5216, Grenoble Alpes University, Saint-Martin-d'Hères, France*
[2]*LEGI, UMR CNRS 5519, Grenoble Alpes University, Saint-Martin-d'Hères, France*
[3]*LPNC, UMR CNRS 5105, Grenoble Alpes University, Saint-Martin-d'Hères, France*

(Received 27 July 2018; revised 27 March 2019; accepted 7 April 2019; published online 30 April 2019)

Simulations of waveguide acoustics require a description of the boundary condition at the open end. For problems involving higher order transverse modes, it is often described by a multimodal radiation impedance matrix. Expressions for the computation of this matrix for an infinite flange condition are available only for circular and rectangular cross-sectional shapes. Thus, a general expression valid for arbitrary cross-sectional shapes is of interest. Such an expression is proposed, validated against known cases, and applied to an arbitrary cross-section shape. The solution is shown to be computationally efficient. © *2019 Acoustical Society of America*.
https://doi.org/10.1121/1.5099262

[MJW] Pages: 2561–2564

I. INTRODUCTION

At the open end of a waveguide, the acoustic boundary condition can be described by a multimodal radiation impedance matrix **Z** which relates the acoustic pressure to the acoustic flow velocity. Such a description relies on the projection of the acoustic field on the transverse mode series ψ_m resulting as a solution of the two-dimensional Helmholtz equation.

The multimodal radiation impedance matrix of a waveguide terminated in an infinite baffle can be obtained in the case of circular[1–3] or rectangular[4] cross-sections from dedicated expressions. However, no general expression is available for an arbitrary cross-section shape.

The purpose of this work is therefore to propose a general numerical expression approximating the radiation impedance matrix for a waveguide with arbitrary cross-sectional shape terminated in an infinite baffle. The expression can be computed from the transverse modes obtained by solving the two-dimensional Helmholtz equation on the cross-sectional shape. The expression is detailed in Sec. II and in Sec. III it is validated against known expressions and applied to an arbitrary cross-sectional shape.

II. NUMERICAL APPROXIMATION OF THE RADIATION IMPEDANCE MATRIX

The radiation impedance matrix **Z** of a waveguide terminated in an infinite baffle, in which the acoustic field can be decomposed over the transverse mode series ψ_n, can be expressed with an implicit time convention $e^{j\omega t}$ as the double surface integral[3,4]

$$Z_{mn} = \frac{j\omega\rho}{2\pi S^2}\int_S\int_{S'} \psi_m(x_1', x_2')\psi_n(x_1, x_2)\frac{e^{-jkh}}{h}dSdS', \qquad (1)$$

with $\omega = 2\pi f$ the angular frequency, f the frequency, wavenumber $k = \omega/c$, ρ the density of the fluid taken as air, S the cross-sectional area, and $h = \sqrt{(x_1 - x_1')^2 + (x_2 - x_2')^2}$ the Euclidean distance between two different locations, (x_1', x_2') and (x_1, x_2), on the cross-sectional surface in a Cartesian coordinate system and with $h \neq 0$.

The transverse modes ψ_m are part of an orthogonal basis and they satisfy the normalization condition

$$\int_S \psi_m^* \psi_n dS = S\delta_{m,n}, \qquad (2)$$

with the Kronecker function $\delta_{m,n}$. Describing the open end boundary condition this way avoids simulating the outward wave propagation. This allows one to limit the computational domain to the internal part of the waveguide, and hence to reduce the computational time and resources.

This expression can be numerically integrated[5] by computing the values of ψ_m and ψ_n on a Cartesian grid of N points and approximating the integrals of Eq. (1) by finite Riemann summations[5]

$$Z_{mn} = \frac{j\omega\rho}{2\pi N^2}\sum_{a=1}^{N}\sum_{b=1}^{N}\psi_m(x_{1a}', x_{2a}')\psi_n(x_{1b}, x_{2b})\frac{e^{-jkh_{ab}}}{h_{ab}}, \qquad (3)$$

with $h_{ab} = \sqrt{(x_{1b} - x_{1a}')^2 + (x_{2b} - x_{2a}')^2}$ and $h_{ab} \neq 0$.

In Eq. (3), the necessity to satisfy the condition $h_{ab} \neq 0$ compromises the accuracy of the computation. In order to work around this limitation, the points on which the amplitude of one of the transverse modes, ψ_m in this case, is computed and distributed in a polar grid of coordinates (r, θ) (see Fig. 1). A new polar grid, represented by dots in Fig. 1, is generated for each point (x_1, x_2) of the Cartesian grid. The radial and angular spacing of this grid are chosen so that the distance between the more external points is of the same order of magnitude as the Cartesian grid spacing. This yields a number of points N_p of the polar grid slightly higher than

a)Electronic mail: remi.blandin@gmail.com

the one of the Cartesian grid N. The origin of the polar landmarks is set on the points (x_1, x_2) so that the radial coordinate is equal to h which can be expressed as r. Thus, the origin is moved for each point (x_1, x_2) expressed in Cartesian coordinates. In this case, the infinitesimal area element is expressed as $dS = rdrd\theta$ in the polar landmarks, and Eq. (1) becomes

$$Z_{mn} = \frac{j\omega\rho}{2\pi S^2}\int_S\int_S \psi_m(r,\theta)\psi_n(x_1,x_2)e^{-jkr}drd\theta dx_1 dx_2. \tag{4}$$

Thus, the division by h, which implies the condition $h \neq 0$ for Eq. (1), is avoided.

Because a regular Cartesian discretization over x_1 and x_2 induces an irregular discretization over r and θ, it is necessary to generate the second grid of N_p points regularly spaced over r and θ. This insures that the area element dS can be expressed as $hdrd\theta$ for each point (r_b,θ_b) and that the proposed simplification can be applied. As a consequence, a new grid is generated for each point (x_{1a}, x_{2a}) and discretization of Eq. (4) yields

$$Z_{m,n} = \frac{j\omega\rho}{2\pi N}\sum_{a=1}^{N}\frac{1}{\sum_{b=1}^{N_p} h_{ab}} \times \sum_{b=1}^{N_p}\psi_m(r_b,\theta_b)\psi_n(x_{1a},x_{2a})e^{-jkh_{ab}}. \tag{5}$$

One must divide the polar coordinate summation by $\sum_{b=1}^{N_p} h_{ab}$ for each value of a as a discretization of $\int_S hdrd\theta$.

III. VALIDATION AND APPLICATION

In order to validate the numerical method described in Sec. II, its outcomes are compared to values obtained with known expressions given by Zorumski[3] and Kemp *et al.*[4] All the mode shapes and cutoff wavenumbers presented hereafter are computed under the assumption of a hard wall boundary condition. The integrals of these expressions are computed with a standard trapezoidal method.[5]

The radiation impedance matrix is computed for all transverse modes whose product $k_c l$ of the cutoff wavenumber k_c and half of the square root of the cross-sectional area[6] $l = \sqrt{S}/2$ yields less than 10. A non-dimensional grid density $\sigma = D/dx_{1,2}$, with $dx_{1,2} = dx_1$ or $dx_{1,2} = dx_2$ and D taken as the smallest distance between the shape's boundary and its center, is used to characterize the accuracy of the approach. Defining σ as a function of D rather than of a characteristic length of the cross-section shape, e.g., radius of the circle or side length of the square, improves the homogeneity of the accuracy obtained with different shapes. The data computed by the numerical method (5) and the expression given by Kemp *et al.*[4] are normalized by $\rho c/S$ since this normalization is applied in the expression given by Zorumski[3] with air sound velocity $c = 343$ m/s (corresponding to a temperature of 20 °C).

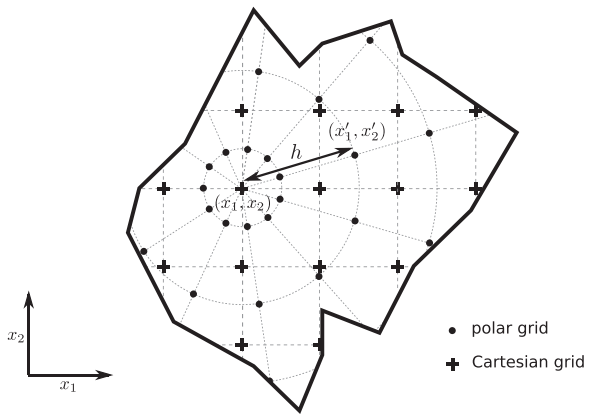

FIG. 1. Simultaneous Cartesian and polar discretization of the cross-sectional surface at point (x_1, x_2).

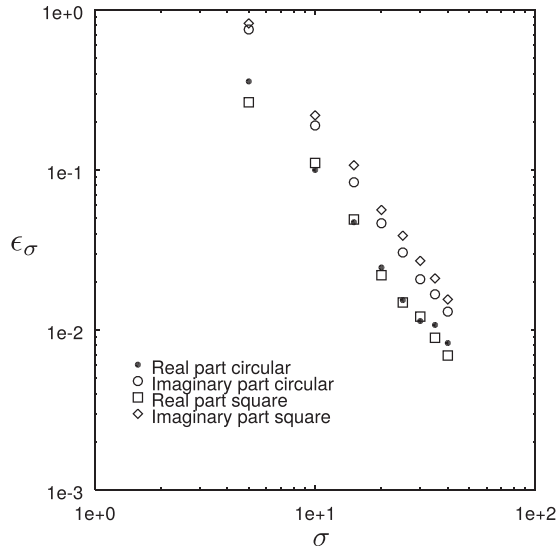

FIG. 2. Maximal term by term error ϵ_σ between the radiation impedance matrices computed numerically and with the expressions provided by Zorumski (Ref. 3) and Kemp *et al.* (Ref. 4) as a function of the non-dimensional grid density σ for circular and square cross-sectional shapes.

The error ϵ_σ for a given value of σ is computed as the maximal term by term difference between the radiation impedance matrices $\mathbf{Z}^\sigma$ obtained with Eq. (5) and $\mathbf{Z}$ from the specific expressions,[3,4]

$$\epsilon_\sigma = \max(|\mathrm{Re}(\mathbf{Z}^\sigma) - \mathrm{Re}(\mathbf{Z})|) + j\max(|\mathrm{Im}(\mathbf{Z}^\sigma) - \mathrm{Im}(\mathbf{Z})|),$$

where Re and Im are the real and imaginary parts, respectively. The variation of the error ϵ_σ with the density σ is

TABLE I. Parameters α and β of the model $f(\sigma) = \alpha\sigma^{-\beta}$ fitted on the error ϵ_σ shown in Fig. 2 between the radiation impedance matrices $\mathbf{Z}^\sigma$ computed for various grid densities σ and $\mathbf{Z}$ from the dedicated expressions (Refs. 3 and 4).

Shape	Part	α	β
Circular	Real	6.8	1.9
	Imaginary	17	2.0
Square	Real	5.9	1.8
	Imaginary	18	1.9

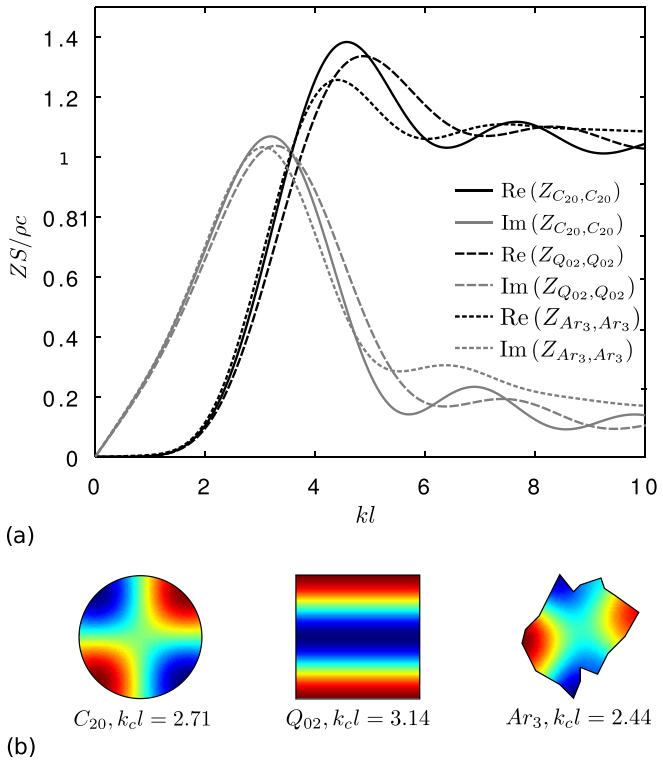

FIG. 3. (Color online) (a) Normalized diagonal terms of the radiation impedance matrix **Z** of the modes C_{20}, Q_{02}, and Ar_3 as a function of normalized wavenumber kl (b) modes shapes of C_{20}, Q_{02}, and Ar_3 and normalized cutoff wavenumbers $k_c l$.

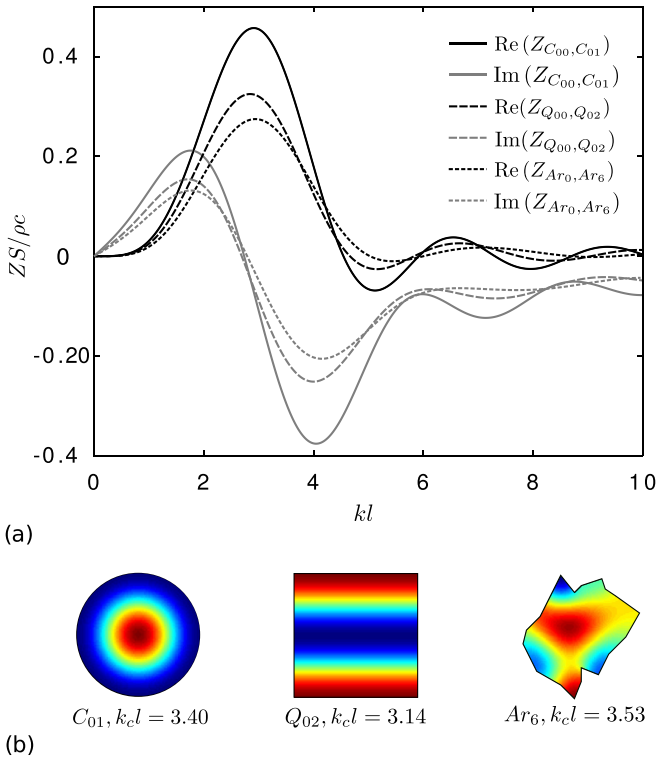

FIG. 4. (Color online) (a) Normalized coupling terms of the radiation impedance matrix **Z** between the plane mode and the modes C_{01}, Q_{02}, and Ar_6 as a function of normalized wavenumber kl (b) modes shapes C_{01}, Q_{02}, and Ar_6 and normalized cutoff wavenumbers $k_c l$.

presented in Fig. 2. One can see that the numerical computation converges towards the known solutions. A model of the type

$$f(\sigma) = \alpha\sigma^{-\beta},$$

with parameters α and β is fitted with linear regression to the variations of the real and imaginary part of ϵ_σ in order to estimate the rate of convergence. All the correlation coefficients obtained for these fits are superior to 0.99, indicating a good correlation. The coefficients α and β thus obtained are presented in Table I.

One can see that α is higher for the imaginary part, indicating an error slightly more important for the imaginary part which can be seen as a shift between $\mathrm{Re}(\epsilon_\sigma)$ and $\mathrm{Im}(\epsilon_\sigma)$ in Fig. 2. The coefficient α is very close to 2 for both a circular and square cross-section shape, indicating a global second order convergence rate, i.e., decay of the error on the order of σ^{-2} for this method.

The proposed method is applied to the case of the arbitrary shape depicted in Fig. 1. The transverse modes Ar_m are computed using finite differences on the same Cartesian grid.[7] The mode shapes C_{mn}, Q_{mn} corresponding to a circular and a square cross-sectional shape, respectively, are computed which specific expressions which can be found in classical textbooks.[8] All shapes have the same cross-sectional area.

The real and imaginary parts of the diagonal terms of **Z** for transverse modes having two nodal lines $Z_{C_{20},C_{20}}$, $Z_{Q_{02},Q_{02}}$, and Z_{Ar_3,Ar_3} are presented in Fig. 3(a) as a function of normalized wavenumber kl. The mode shapes and normalized cutoff wavenumbers $k_c l$ corresponding to these modes (C_{20}, Q_{02}, and Ar_3) are presented in Fig. 3(b). The radiation impedance of the three shapes is very similar up to k_{cl}. Above this value ($kl > k_c l$), the cross-sectional shape induces differences in losses (real part) and phase shift (imaginary part).

The coupling terms of **Z** between the plane mode ($k_c = 0$) and transverse modes C_{01}, Q_{02}, and Ar_6 are plotted in Fig. 4(a). The corresponding mode shapes and normalized cutoff wavenumbers $k_c l$ are presented in Fig. 4(b). Important differences can be observed for almost the whole wavenumber range.

IV. CONCLUSION

A general numerical expression is proposed for the computation of the multimodal radiation impedance matrix of a waveguide with arbitrary cross-sectional shape. The problem of the singularity at the point (0, 0) is treated through the simultaneous use of two different grids of points regularly spaced in a Cartesian and a polar coordinate system, respectively. The convergence of the method is on the order of σ^{-2}, which confirms the interest from a computational point of view. Application to different shapes including an arbitrary one shows the relevance of computing shape-specific radiation impedances rather than relying on approximations.

[1]W. Duan, R. Kirby, J. Prisutova, and K. V. Horoshenkov, "Measurement of complex acoustic intensity in an acoustic waveguide," J. Acoust. Soc. Am. **134**, 3674–3685 (2013).

[2]A. Snakowska, J. Jurkiewicz, and Ł. Gorazd, "A hybrid method for determination of the acoustic impedance of an unflanged cylindrical duct for multimode wave," J. Sound Vib. **396**, 325–339 (2017).
[3]W. Zorumski, "Generalized radiation impedances and reflection coefficients of circular and annular ducts," J. Acoust. Soc. Am. **54**, 1667–1673 (1973).
[4]J. A. Kemp, D. M. Campbell, and N. Amir, "Multimodal radiation impedance of a rectangular duct terminated in an infinite baffle," Acta Acust. Acust. **87**(1), 11–15 (2001).
[5]P. J. Davis and P. Rabinowitz, *Methods of Numerical Integration* (Academic, New York, 1984), Chap 2, pp. 51–198.
[6]The values of this parameter differ from the non-dimensional cutoff frequencies (Helmholtz numbers $He = k_c a$, where a is the duct radius) commonly applied in the circular duct theory.
[7]I. Singer and E. Turkel, "High-order finite difference method for the Helmholtz equation," Comput. Methods Appl. Mech. Eng. **163**, 343–358 (1998).
[8]P. M. Morse and K. U. Ingard, *Theoretical Acoustics* (Princeton University, Princeton, NJ, 1986), Chap. 9, pp. 503–510.